A TWO-SCALE APPROXIMATION FOR EFFICIENT REPRESENTATION OF NONLINEAR ENERGY TRANSFERS IN A WIND WAVE SPECTRUM

by

Donald T. Resio[1]
William Perrie[2]
[1]ERDC-Coastal and Hydraulics Lab, USA
[2]Fisheries & Oceans Canada, BIO, Dartmouth, Nova Scotia, Canada

Abstract

Following a discussion of shortcomings within existing methods for efficiently estimating transfer rates in wind wave spectra due to four-wave interactions, a new method for estimating these transfer rates is derived and tested. This formulation is based on a two-scale approximation (TSA) to the total integral. Comparisons of this new estimation method to the full integral are given for the several idealized spectra, including JONSWAP spectra with different peakednesses, a finite depth case, and cases with perturbations added to underlying parametric spectra. In particular, these comparisons show that the TSA is a significant improvement in accuracy over the Discrete Interaction Approximation in deep water and an even greater improvement in accuracy in shallow water.

1. Introduction

Hasselmann and Hasselmann (1985), and Hasselmann et al. (1985) argued that, to achieve a proper detailed-balance formulation for the physics of wave generation, it was essential to retain the same number of degrees of freedom within all source terms as contained in the modeled directional spectrum. They opined that models failing to adhere

to this criterion would not be able to adapt to complex situations and would require extensive local tuning in applications.

In a detailed-balance wave model, each of the three main source terms believed responsible for wave generation and decay (typically wind input (S_{in}), nonlinear wave-wave interactions (S_{nl}), and wave breaking (S_{ds})) must be cast in a detailed-balance form. Hasselmann et al (1985) and Komen et al. (1984) noted that S_{in} and S_{ds} could be straightforwardly written in detailed-balance forms. However, no detailed-balance form for S_{nl} existed at that time, other than the full integral representation, which even today is considered much too cumbersome for operational wave modeling.

To fill this void, Hasselmann et al (1985) formulated the Discrete Interaction Approximation, commonly referred to as the DIA. This important advance allowed all three primary source terms to be written in a detailed-balance form, leading to a new generation of wave models, termed third-generation (also denoted 3G) wave models (Komen et al., 1994). Unfortunately, due to practical constraints on computations within operational models, the formulation of the DIA restricted possible four-wave interactions to a subset in which two of the interacting waves are co-located. This subset represents only a small portion of the total interactions included within the general interaction space; consequently, the DIA is not able to provide a consistent representation for S_{nl} when compared to the full integral solution. Instead, the DIA was calibrated to match only a single parametric quantity, the integrated energy transfer rate onto the forward face of the

spectrum for a standard JONSWAP spectrum (Hasselmann et al, 1973), since this quantity is of primary importance in wave generation.

Since the standard JONSWAP spectral form will be utilized in several subsequent comparisons and discussions it is given here for reference,

$$E(f) = \frac{\alpha g^2}{(2\pi)^4} f^{-5} \exp\left[-1.25 \left(\frac{f}{f_p} \right)^4 \right] \gamma^{\Theta}$$

where $E(f)$ is the spectral energy density at f,

$$\Theta = \exp\left[\frac{-(f - f_p)^2}{2\sigma^2 f_p^2} \right] \qquad (1)$$

and

$\sigma = \sigma_a$ for $f < f_p$

$= \sigma_b$ for $f \le f_p$

This spectral characterization has five parameters, the spectral peak frequency (f_p), the equilibrium range coefficient for an f^{-5}-based spectrum (α), peakedness (γ), the spectral width for frequencies less than the spectral peak frequency (σ_a), and the spectral width for frequencies greater than or equal to the spectral peak frequency (σ_b).

Young and Van Vledder (1993) have shown that the nonlinear source term (S_{nl}) is of central importance to the wave generation process; thus, the current state of the art in wave modeling via third-generation models can be significantly impaired by the lack fidelity in the DIA. Consistent with this expectation, considerable evidence has now accumulated showing that third-generation models do not yield appropriate results for situations where

winds blow at oblique angles near a coast or for the case of narrow water bodies (Donelan, 1980; Donelan et al, 1985; Pettersson et al, 2004).

2. Estimation of the nonlinear interaction source term

Hasselmann (1962) and Zakharov and Filonenko (1966) established the theoretical foundation for four-wave interactions within wave spectra. Webb (1978), for the deep-water case, and Resio *et al* (2001), for finite depth, formulated representative solutions for the transfer integral that have been shown to provide reasonable numerical representations for transfer rates due to these interactions. In general, accurate estimation of S_{nl} for each frequency-direction component within a spectrum requires the evaluation of $N_1 N_2 N_3$ contributing elements, where N_1 is the number of discretized frequency bands in the spectrum, N_2 is the number of discretized angles in the spectrum, and N_3 is the number of sample points along the interaction locus (Resio and Perrie, 1991). Hence the number of contributions that must be considered over the entire spectrum will be on the order of $N_1^2 N_2^2 N_3$. A typical operational wave model uses 20 to 25 frequencies and 24 to 32 angle bands. Resio and Perrie (1991) showed that about 30 points along the wave-wave locus of interactions are required to provide an accurate estimate for the full integral. Even with judicious filtering of regions included within the integrand, the number of operations required for a quasi-exact representation of S_{nl} is expected to remain much too large to allow its effective application in practical wave modeling, for some time to come.

At least five different approaches have been made to formulate an accurate, efficient evaluation of the full Boltzmann integral solution for nonlinear transfers in a wave spectrum: 1) parametric representations (Barnett, 1968; Ewing, 1971; Resio, 1981, Hasselmann et al, 1985); 2) local interaction or diffusion operator approximations (Hasselmann et al, 1985; Polnikov, 2002; Pushkarev et al, 2004); 3) linear combinations of orthogonal functions (Hasselmann et al, 1985); 4) reduced integration domains (Lin and Perrie, 1997, 1999); and 5) the discrete interaction approximation, or DIA. Of these, only the DIA has found much success within operational wave models; consequently, this is the only method that will be examined here for contrast with the TSA.

In Figure 1, the DIA estimate for S_{nl}, as optimized by Hasselmann et al (1985), is compared to the full Boltzmann integral estimate of S_{nl} for a standard JONSWAP spectrum (peakedness parameter, γ, equal to 3.3), with a $\cos^4\theta$ angular distribution of energy around the central wave direction. The directionally integrated transfers from the DIA are calibrated to optimize agreement with the full integral solution for the forward face of the spectrum, but deviate substantially elsewhere within the spectrum. Comparisons of the DIA performance relative to the full integral solution, for spectra other than the standard JONSWAP peakedness, typically exhibit substantially larger deviations than shown in Figure 1. For example, Figures 2 and 3 provide comparisons of the DIA to the full integral for cases with the JONSWAP peakedness parameter equal to 1 and 7, respectively. Thus, although the DIA's calibration for γ equal to 3.3 forces some degree of consistency between it and the full integral, for $\gamma = 3.3$, this agreement is limited to a small range of γ

values centered on this value and cannot be construed as representing a general validation for a broad range of spectral shapes.

In particular, as a "fully-developed" spectral shape (γ =1) is approached, one must assume a large dissipative wave-breaking term near the spectral peak to balance DIA's substantial over-estimation of the nonlinear wave-wave interactions on the forward face of the spectrum to arrest wave growth at this stage. Moreover, the corresponding wind input source term would need to be artificially enhanced on the rear face of the spectrum for essentially all cases in order to compensate for the DIA's tendency to overestimate the magnitude of the negative lobe in this spectral region.

The primary reason for the DIA's failure to provide suitable estimates for S_{nl} is most likely due to the difference between the DIA's integration locus, which falls only along the Phillips (1960) figure-8 diagram; whereas, the full integral includes contributions from the entire area surrounding any point within a continuous spectrum. This lack of consistency between the integration domains is the primary reason why adding more quadraplets along the figure 8 does not produce a very marked improvement in the DIA formulation compared to the total Boltzmann integral.

Given today's focus on coastal environments, it is also important that the operational form for S_{nl} provide accurate estimates for relatively shallow depths. The method for estimating S_{nl} in today's 3G shallow water models (Booij et al., 1999) is based on a scaling argument initially developed by Herterich and Hasselmann (1980). As pointed out by

Herterich and Hassemann (1980), this formulation is limited in its applicability to wave spectra for which $k_p h \geq 1$, where k_p is the wavenumber of the spectral peak.

To investigate what happens when the restriction on $k_p h \geq 1$ is violated, let us examine the simple case of a standard JONSWAP spectrum (the calibration case for the DIA) with a peak period of 10 seconds in a depth of 10.5 meters ($k_p h \approx 0.7$). Figure 4 shows a comparison of a scaled DIA calculation and the full-integral, finite-depth calculation for the same spectrum. The scaled DIA estimate underestimates the positive lobe on the forward face of the spectrum by about one order of magnitude. It also underestimates the magnitude of the central negative lobe in S_{nl} by a factor of about 6 and moves this lobe from the spectral peak region to higher frequencies. Importantly, since the Herterich and Hasselmann (1980) scaling provides only a scalar multiplier for the entire range of frequencies in the spectrum, it does not allow the spectral shape to evolve from its deep-water form into the finite-depth form. This evolution has been well documented by Bouws et al. (1985) who linked changes in spectral form to significant energy losses within coastal wave spectra and is consistent with the pattern of nonlinear interactions in finite depth as shown by Resio et al. (2001).

3. A two-scale approximation (TSA) for nonlinear transfers

Hasselmann (1962) showed that the cumulative transfer of energy in a continuous spectrum from one spectral frequency-direction component to another in deep water

involves four interacting waves, located at wavenumbers $\underline{k}_1, \underline{k}_2, \underline{k}_3, \underline{k}_4$. Following Webb (1978), the rate of change of action density at a point within a spectrum, $\underline{k}_1$, can be written as an integral, over all $\underline{k}_3$, of the transfer rates $T(\underline{k}_1, \underline{k}_3)$ from wavenumber $\underline{k}_3$ to wavenumber $\underline{k}_1$, i.e.

$$\frac{\partial n(\underline{k}_1)}{\partial t} = \iint T(\underline{k}_1, \underline{k}_3) d\underline{k}_3 \tag{2}$$

. Webb (1978) showed that the transfer rate depends on action densities at all four interacting wavenumbers and could be written as

$$T(\underline{k}_1, \underline{k}_3) = \iint [n_1 n_3 (n_4 - n_2) + n_2 n_4 (n_3 - n_1)] C(\underline{k}_1, \underline{k}_2, \underline{k}_3, \underline{k}_4) \theta\left(|\underline{k}_1 - \underline{k}_4| - |\underline{k}_1 - \underline{k}_3|\right) | \frac{\partial W}{\partial \underline{n}} |^{-1} \, d\underline{s} \tag{3}$$

where $\theta(x) = 1$ if $x > 0$ and $\theta(x) = 0$ otherwise, where $\underline{k}_4 = \underline{k}_1 + \underline{k}_2 - \underline{k}_3$ and $\underline{k}_2 = \underline{k}_2\left(s, \underline{k}_1, \underline{k}_3\right)$, and n_i denotes the action density at $\underline{k}_i$. The function W defined as

$$W = \omega_1 + \omega_2 - \omega_3 - \omega_4 \tag{4}$$

constrains the interactions to ensure energy conservation, $\underline{s}$ is the locus of points satisfying the condition W=0, and $\underline{n}$ is the local orthogonal to the resonant locus. Webb (1978)'s derivation utilized the deep-water dispersion relationship,

$$\omega_i^2 = gk_i \tag{5}$$

where $k_i = |\underline{k}_i|$. However, Resio et al. (2001) showed that the equation (3) was valid in shallow water, provided the general form of the dispersion relationship was used,

$$\omega_i^2 = gk_i \tanh(k_i h) \tag{6}$$

where h is the water depth, along with the appropriate depth-dependent forms for the coupling coefficient.

The lack of success in various previous approximations to the full-integral for nonlinear energy transfers in deep-water ocean spectra stems from several factors, including, 1) the relatively broad structure of the transfer function, $T(\underline{k}_1, \underline{k}_3)$ in equation 3, 2) the existence of strong localized interaction areas within these broad patterns, which can be very important near the peak of the spectrum, 3) the variation of the shape and location of the regions of strong interactions within a spectrum, and 4) the cubic dependence of the interaction rates on local energy densities. In addition to these deep-water problems, it does not appear possible to find a simple scalar multiplier suitable for transforming estimates of nonlinear transfers in deep water to "equivalent" estimates in shallow water. Thus, it seems that a totally new approach is required.

We begin by splitting the action density terms, n_i, in equation 3 as the sum of two arbitrary components

$$n_i = \hat{n}_i + n_i'$$

where the "hat" $\hat{n}_i$ represents the first component, and the "prime" n_i' represents the second. For this two-component decomposition, the density term in the transfer integral becomes

$$\begin{aligned} N^3 = {} & \hat{n}_1\hat{n}_3(\hat{n}_4 - \hat{n}_2) + \hat{n}_2\hat{n}_4(\hat{n}_3 - \hat{n}_1) + \\ & n_1'n_3'(n_4' - n_2') + n_2'n_4'(n_3' - n_1') + \\ & \hat{n}_1\hat{n}_3(n_4' - n_2') + \hat{n}_2\hat{n}_4(n_3' - n_1') + \\ & n_1'n_3'(\hat{n}_4 - \hat{n}_2) + n_2'n_4'(\hat{n}_3 - \hat{n}_1) + \\ & \hat{n}_1n_3'(\hat{n}_4 - \hat{n}_2) + \hat{n}_2n_4'(\hat{n}_3 - \hat{n}_1) + \\ & n_1'\hat{n}_3(\hat{n}_4 - \hat{n}_2) + n_2'\hat{n}_4(\hat{n}_3 - \hat{n}_1) + \\ & \hat{n}_1n_3'(n_4' - n_2') + \hat{n}_2n_4'(n_3' - n_1') + \\ & n_1'\hat{n}_3(n_4' - n_2') + n_2'\hat{n}_4(n_3' - n_1') \end{aligned} \qquad (7)$$

It can be seen here that the general integral can be written as the sum of interactions among the first component $\hat{n}_i$ terms only (row 1), interactions among the second component n_i' terms only (row 2), and cross interactions among the two components (rows 3-8). If the two components are of comparable magnitude everywhere, each row in equation 7 will also be of comparable magnitude everywhere. In this case the cross-interactions will be six times larger than either the interactions involving $\hat{n}_i$ terms alone or the interactions involving n_i' terms alone.

Substituting the form for the spectral density from equation 7 into equation 3 does not reduce the accuracy of the transfer integral and affords a good means to examine the general problem of two arbitrary interacting wave trains. Although this can also be done numerically by subtracting the interactions for a single wave train from the interactions for the sum of two wave trains, the latter approach does not provide the same insight as the use of the "split" density function, where the cross-interaction terms can be examined algebraically. However, this is beyond the focus of this paper, so we shall not examine this aspect of the approach used here.

Although substitution of the two-component spectrum ($\hat{n}_i$ and n_i') into the density triplets provides a convenient methodology for examining interactions between two wave fields, it requires more computational operations than the simple density form n_i to compute the full integral. Thus, *per se*, such a partitioning does not provide an effective tool for efficiently estimating nonlinear transfer rates. To accomplish this, we will assume that the distribution of energy within a spectrum can be expressed as the sum of two primary scales (thus the Two Scale Approximation name), a broad-scale variation that can be captured parametrically, and a local-scale variation that represents deviations between the parameterized action density levels and the actual action densities within a spectrum.

The TSA retains the effect of the overall spectral shape on nonlinear transfers, while allowing the effects of localized deviations and the interactions between the deviations and the large-scale spectral structure to be included. Inclusion of only the first term, $\hat{n}_i$, is comparable to older parametric methods, which, as noted previously, would result in

artificial constraints on the behavior of the spectrum if only this term were retained. Inclusion of the second (local) scale, n_i' , retains the same number of degrees of freedom as the number of discretized spectral elements.

In general, we can write the total interactions for any two-part spectral decomposition of the type introduced here ($\hat{n}_i$ and n_i') as

$$S_{nl}(f,\theta) = B + L + X \tag{8}$$

where *B* and *L* represent interactions within the broad-scale only energies $\hat{n}_i$ and the local-scale only energies n_i', respectively, and *X* represents the cross-interactions between the two scales. Using the "exact" integral we can generate a matrix of detailed estimates of S_{nl} for a set of *n* parameters,

$$S_{nl}(f,\theta)_{broad-scale} = B(f,\theta,x_1,...,x_n) \tag{9}$$

where x_i is the value of the i^{th} parameter. The crux of the remaining problem in estimating $S_{nl}(f,\theta)$ via the TSA formulation is to find a suitable approximation for $L + X$.

The complete transfer integral can be separated into the sum of seven separate integrals, each containing only a single row of equation 7 within its density function, plus the broad-scale contribution, i.e.

$$S_{nl} = B + \sum_{j=2}^{8} \iint N_j^3 C \, | \frac{\partial W}{\partial n} |^{-1} \, ds \; k_3 d\theta_3 dk_3 \qquad (10)$$

where *j* refers to the j^{th} row in equation 7. If all seven terms inside the sum (j = 2, 8) were computed, this would represent an approximate seven-fold increase in the number of computer operations required compared to the initial integral form, for an "*exact*" representation. However, since local-scale perturbations (n_i' terms) represent deviations around the broad-scale basis ($\hat{n}_i$ terms), it is expected that n_2' and n_4', along with their differences and their products, will contain both positive and negative regions as one moves along the respective interaction locus for each. On the other hand, the broad scale terms $\hat{n}_2$ and $\hat{n}_4$ tend to have much longer lengths along $\underline{s}$ in which the sign is unchanged. And, , if we have done our parameterization in a reasonable way, the magnitude of the local-scale terms , n_2' and n_4', tends to be substantially smaller than that of the broad-scale terms, $\hat{n}_1$ and $\hat{n}_3$. Consequently, all rows and parts of rows containing n_2' and n_4' in equation 7, will tend to be significantly smaller those containing $\hat{n}_2$ and $\hat{n}_4$, as well as those containing $\hat{n}_1$ and $\hat{n}_3$, and therefore will be neglected in the TSA formulation.

After eliminating terms containing n_2' and n_4' and simplifying, it is possible to write equation 10 as

$$\frac{\partial n_1}{\partial t} = B + \iint N_*^3 C \,|\frac{\partial W}{\partial n}|^{-1}\, ds\; k_3 d\theta_3 dk_3 = B + (L + X)_* \qquad (11)$$

where N_*^3 is given by

$$N_*^3 = \hat{n}_2 \hat{n}_4 (n_3' - n_1') + n_1' n_3' (\hat{n}_4 - \hat{n}_2) + \hat{n}_1 n_3' (\hat{n}_4 - \hat{n}_2) + n_1' \hat{n}_3 (\hat{n}_4 - \hat{n}_2) \qquad (12)$$

The subscript "*", after the parenthesis in equation 11, indicates that the L- and X-scale interaction terms include only the density terms given in equation 12.

Since both $\hat{n}_2$ and $\hat{n}_4$ depend only on the same broad-scale set of parameters $(x_1, ..., x_n)$ used in calculating B, this same set can be used as the basis for computing all line integral quantities involving $\hat{n}_2$ and $\hat{n}_4$ in equation 11. It can be seen from equation 12 that this representation retains all broad-scale terms in the density equation and is therefore an "exact" solution for the parametric portion of the spectrum. The local- and cross-scale interactions retain only the set of densities that neglect contributions due to n_2' and n_4'.

Making use of wavenumber and angle scaling relations and inherent steepness scaling, we can write equation 12 as

$$\frac{\partial n_1}{\partial t} = \left(\frac{\beta}{\beta_0}\right)^3 B + \left(\frac{f_{p_0}}{f_p}\right) \left\langle \begin{array}{r} \left(\frac{\beta}{\beta_0}\right) \iint (\hat{n}_1 n_3' + n_1' \hat{n}_3 + n_1' n_3') \Lambda_p (\hat{n}_2 - \hat{n}_4, \underline{k}_1, k_*, \theta_*, \mathrm{x}_1, ..., \mathrm{x}_n)\, k_* d\theta_* dk_* \\ + \left(\frac{\beta}{\beta_0}\right)^2 \iint (n_1' - n_3') \Lambda_d (\hat{n}_2 \hat{n}_4, \underline{k}_1, k_*, \theta_*, \mathrm{x}_1, ..., \mathrm{x}_n)\, k_* d\theta_* dk_* \end{array} \right\rangle$$

where

$$\Lambda_p (\hat{n}_2 - \hat{n}_4, \underline{k}_1, k_*, \theta_*, \mathrm{x}_1, ..., \mathrm{x}_n) = \oint C \left| \frac{\partial W}{\partial n} \right|^{-1} (\hat{n}_4 - \hat{n}_2) ds$$

$$\Lambda_d (\hat{n}_2 \hat{n}_4, \underline{k}_1, k_*, \theta_*, \mathrm{x}_1, ..., \mathrm{x}_n) = \oint C \left| \frac{\partial W}{\partial n} \right|^{-1} \hat{n}_2 \hat{n}_4 ds$$

(13)

and where $\left(\frac{\beta}{\beta_0}\right)$ is the ratio of the actual steepness to a reference steepness for the large-scale spectral component, $\left(\frac{f_{p_0}}{f_p}\right)$ is the ratio of the reference spectral peak frequency to the actual peak frequency of the spectrum, and θ_* and k_* are defined as

$$\theta_* = \theta_3 - \theta_1 \tag{14}$$

and

$$k_* = \left(\frac{k_3 - k_1}{k_p}\right) \tag{15}$$

An important computational advantage of equation 13 is that, even though both local-scale and cross interaction contributions to the transfer integral are retained, all terms

involving the line integral along $\underline{s}$ can be pre-computed on the same discretized basis as B. Integration around these loci constitutes the innermost loop for computations within the WRT formulation. Numerical experiments show that this innermost loop represents between 99.5% and 99.7% of the total computation time in a recently optimized WRT code for most spectra. Retaining the same integration domain as the complete integral therefore can reduce the time required for computations by about a factor of 250 to 500. Additional reductions in TSA run time can be achieved by 1) limiting the number of points at which S_{nl} is evaluated and 2) limiting the integration domain via restrictions on k_* and θ_*.

4. Tests of the TSA for parametric spectra

A number of tests are required to establish the viability of the TSA formulation for spectral wave modeling. Following the approach of the initial paper on the DIA by Hasselmann et al. (1985), the first tests will be limited to static comparisons between the TSA and the full integral solution for nonlinear transfers in deep water. From the structure of equation 13, it is apparent that the accuracy of the parameterization used for *B* will directly influence the accuracy of this approximation. Since the purpose of this paper is to introduce the two-scale approximation and to demonstrate its relevance for wave modeling, we shall use only a simple parameterization here.

Let us assume that a simple characterization of the broad-scale structure of deep-water wave spectra can be accomplished by five parameters, f_p, β, κ, σ_a, and σ_b where these are defined as the spectral peak frequency, equilibrium range coefficient, f^{-4}-based

peakedness parameter, spectral width parameter for the forward face of the spectrum (low-frequency side of the spectral peak), and the spectral width parameter for the rear face of the spectrum (high-frequency side of the spectral peak). It is possible to show, both analytically and numerically, that wave-wave interactions for two f^{-4} spectra as defined here, with the same values for κ, σ_a, and σ_b, along with the same directional distribution of energy are exactly related by

$$\beta^3 f_p^{-1} S'_{nl}(f,\theta) = \beta'^3 f_p'^{-1} S_{nl}(f,\theta) \qquad (16)$$

where the prime is used to denote the values of β and f_p for a second spectrum. Thus, β and f_p can both be algebraically factored out of this type of a parametric representation for a spectrum, while still retaining exact information on nonlinear transfer rates. This scaling, was used in equation 13 to convert from reference values to specific spectra. If we further simplify the parameterization by fixing both spectral width parameters to specific values, the peakedness parameter, κ, is left as the only free parameter in the spectral representation that will be used here. For all tests shown here, all pre-computed terms are retrieved from matrices of the form $B(f,\theta,\kappa)$, $\Lambda_p(f,\theta,\kappa)$, and $\Lambda_d(f,\theta,\kappa)$, with κ discretized in increments of 0.1 over a range of 0.4 to 4.

The JONSWAP spectrum is an f^5-based spectrum rather than an f^4-based spectrum; consequently, tests with this spectral form provide a good test for TSA, since it deviates considerably from the broad-scale spectral form used here. Figures 5, 6, and 7 provide

comparisons of the directionally integrated TSA results to the full-integral solution for JONSWAP spectra with peakednesses equal to 1, 3.3, and 7, respectively. The contribution to the TSA from the parametric solution alone is also shown in these figures. Overall, since these are relatively simple spectra, the basic parametric representation (the interactions among only the *B*-scale spectral components) provides a fairly good approximation to the directionally integrated transfer rates for each spectrum. However, in each case, the addition of the *L*- and *X*-scale terms into the TSA is seen to improve the agreement between the full-integral solution and the approximation.

In the case of the Pierson-Moskowitz spectrum ($\gamma = 1$), the broad-scale solution slightly misplaces the positive transfer lobe toward lower frequencies and overestimates its magnitude by about 50%. The use of additional terms in the TSA formulation moves the positive lobe into very good agreement, in terms of both location and magnitude. In both the negative lobe region and the high-frequency region, the additional terms of the TSA formulation help move the displaced mid-frequency energy sink into closer agreement with the full-integral solution; but the improvement is not as marked as it is for the initial positive lobe.

In the case of the standard JONSWOP spectrum ($\gamma = 3.3$), the additional TSA terms reduce the undershoot of the parameterized solution, relative to the parametric solution alone, in the low-frequency positive lobe, by slightly over 20%, and in the mid-range negative lobe, by slightly over 40%. In the high-frequency region, the full TSA also reduces the deviations from the full-integral solution by over 50%. In the case of the very

peaked spectrum ($\gamma = 7$), the additional TSA terms result in improvements over the parametric (B-scale) solution by magnitudes that are similar to those of the standard JONSWAP spectrum ($\gamma = 3.3$).

Figures 5, 6, and 7 suggest that the TSA could have considerable promise for wave modeling. However, because the *B*-scale interactions represent a significant portion of the total interactions and appear to capture much of the basic shape of the overall transfer function, these cases may not provide a strong argument that this approximation will work well for spectral shapes with significant local deviations from a broad parametric shape. To investigate the suitability of the TSA for more complex spectra, we examine some results for spectra with perturbations added to them. Previous investigations (Perrie and Resio, 2004) have shown that the DIA does an extremely poor job in representing complex cases such as will be examined below.

Using the spectral shape of Resio and Perrie (1989) with an added Gaussian energy perturbation yields an equation of the form

$$E(f,\theta) = \frac{\alpha u_s g f^{-4}}{(2\pi)^3} \Psi_1\left(\frac{f}{f_p}\right) \Psi_2(\theta - \theta_0) \times sZ\left(f - f_z, \theta - \theta z\right) \qquad (17)$$

where the perturbation term is given in terms of a bivariate Gaussian form

$$Z(f-f_z,\theta-\theta_z) = A_z \exp\left(\frac{-\hat{\theta}^2}{2}\right)\exp\left(\frac{-\hat{f}^2}{2}\right)$$

where

$$\hat{\theta} = \frac{(\theta-\theta_z)}{\sigma_\theta} \qquad (18)$$

$$\hat{f} = \frac{f-f_z}{\sigma_f}$$

with parameter values of $f_z = 1.5 f_p,\ \theta_z = \theta_0,\ \sigma_\theta = 0.3,\ \sigma_{\mathrm{f}} = 0.1,$ and $\mathrm{A}_z = 1.0$. In this case the parameterized spectral shape will be taken as the first term in equation 17, leaving the perturbation term exactly equal to the second term multiplied by the local energy density. Figure 8 gives the results for the complete integral solution, the parametric-only interactions, and the TSA for the case of κ = 2.2 (characteristic of a local sea spectrum) and a $\cos^4\theta$ angular spreading function. Since the parameterization does not have any information on the perturbation, it retains precisely the same form as if the positive perturbation did not exist. The addition of the *L*- and *X*-scale interactions in the TSA does an excellent job in capturing the effects of the perturbation. Figure 9 provides results similar to those in Figure 8, for the case of all parameters held the same, except that we change the sign of the perturbation, i.e. $A_z = -1$. Again, the *L*- and *X*-scale interactions do a remarkable job in capturing the effects of the perturbations.

In tests shown in Figures 8 and 9, the central angle of the perturbation is identical to the mean angle of the parametric spectrum. Figure 10 shows the results for a case in which the spectrum contains a 40-degree discontinuity at $f = 1.5 f_p$, retaining the same values for E(f) as though the spectrum had not been shifted. A $\cos^4\theta$ angular spreading function is used for this case and κ = 1.2. In this case, although the TSA captures the magnitudes of

the positive lobes at both the spectral peak and the region immediately above the angular discontinuity along with the positions of these lobes, it overestimates the negative lobe by a factor of about 2. While this performance is still markedly superior to the performance of the DIA for this type of case, we feel that it may be possible to improve upon these results by paying additional attention to the treatment of the *B*-scale interactions, which was intentionally kept quite simple here.

As a final test of the TSA, we shall examine its performance for the same finite-depth case shown previously for the DIA, using exactly the same combination of *B*-scale parameterization and *L*- and *X*-scale interactions as for the deep-water cases. The only difference is that each of the *B*-scale, *L*-scale, and *X*-scale terms were computed using the actual depth of 10.5 meters. In general, for finite-depth applications, a second free parameter ($k_p h$) could be used to represent the B-scale terms quite accurately, based on a suitable discretization. Figure 11 shows the results for the full-integral solution, TSA, and the DIA. It is clear that the TSA has captured the finite-depth effects quite well, and certainly much better than the extrapolation of the Herterich and Hasselmann (1980) approach to values beyond their region of applicability.

5. Discussion and Conclusions

For wave models to accurately represent the detailed-balance of the source terms responsible for wave generation and decay under a wide range of conditions, it is essential

that each of the three primary terms contributing to this balance be realistically depicted for a substantial range of spectral shapes. For over twenty years, the only approximation for four-wave interactions that has shown utility for detailed-balance wave modeling has been the Discrete Interaction Approximation, or DIA. This paper has demonstrated that significant problems exist with the DIA estimates of nonlinear transfers in deep water. These errors cannot be "tuned out" since the DIA is based on a reduced form of the Boltzmann integral that does not include the majority of the actual interactions within a spectrum. In shallow water, the extrapolation of scaling arguments due to Herterich and Hasselmann (1980) into regions well beyond the appropriate range for this approximation renders estimates of nonlinear transfers in detailed-balance models very inaccurate when applied in depths typical of coastal regions.

This paper introduces a new approximation, the Two-Scale Approximation (TSA), based on the separation of a spectrum into a broad-scale component and a local-scale (perturbation) component. This new method relies on a parametric representation of the broad-scale spectral structure, while preserving the degrees of freedom essential to a detailed-balance source term formulation via the inclusion of the second scale in the approximation. This approximation appears to provide significantly increased accuracy over the DIA in all regions of the spectrum for all of the cases examined in this paper. Of particular importance is the very large improvement over the DIA for the finite-depth case examined. It is important to note that this new approximation is based on the actual structure of the full-integral solution and uses no tuning coefficients to achieve the results shown in this paper.

Acknowledgements

Support for this research comes from the U.S. Army Corps of Engineers MORPHOS program, the Canadian Panel on Energy Research and Development (PERD - Offshore Environmental Factors Program), ONR (US Office of Naval Research) through GoMOOS – the Gulf of Maine Ocean Observing System, the **S**outheast University Research Assoc. **C**oastal **O**cean **O**bserving and **P**rediction (SCOOP) program, the Canada Foundation for Climate and Atmospheric Studies and Petroleum Research Atlantic Canada. The authors also wish to acknowledge the Office, Chief of Engineers, U.S. Army Corps of Engineers for permission to publish this paper.

References

Barnett, T.P. 1968: On the generation dissipation and prediction of ocean wind waves. *J. Geophys. Res.* **73**, 513-530.

Booij, N., Ris, R. C., and Holthuijsen, L. H.: 1991: A third-generation wave model for coastal regions, Part I, Model description and validation. *J. Geoph. Res.*, C4, **104**, 7649–7666.

Bouws, E., Gűnther, H., Rosenthal, W., and Vincent, C. L.: 1985: Similarity of the wind wave spectrum in finite dept water, 1, Spectral form. *J. Geophys, Res.*, **C90**, 975-986.

Donelan, M.A., 1980: Similarity theory applied to the forecasting of wave heights, periods, and directions, Proc. Canadian Coastal Conf., April 22, Burlington, Ontario.

Donelan, M. A., J. Hamilton and W. H. Hui, 1985: Directional spectra of wind-generated waves, *Phil. Trans. R. Soc. Lond.*, *A*, **315**, 509-562.

Ewing, J.A., 1971: A numerical wave prediction method for the North Atlantic Ocean. *Dtsch. Hydrogr. Z.* **24**, 241-261.

Hasselmann, K., 1962: On the nonlinear energy transfer in a gravity wave spectrum, Part 1, *J. Fluid Mech.*, **12**, 481–500.

Hasselmann, K., Barnett, T.P., Bouws, E., Carlson, H., Cartwright, D. E., Enke, K., Ewing, J. A., Gienapp, H., Hasselmann, D. E., Kruseman, P., Meerburg, A., Muller, P., Olbers, D. J., Richter, K., Sell W., and Walden, H., 1973: Measurements of wind-wave growth and swell decay during the Joint North Sea Wave Project (JONSWAP), *Ergänzungsheft zur Deutschen Hydrographischen Zeits.*, *12*, *Reihe A8*, 95 pp., 1973.

Hasselmann, S. and Hasselmann, K., 1985: Computations and parametrizations of the nonlinear energy transfer in a gravity wave spectrum, Part I, A new method for efficient computations of the exact nonlinear transfer integral, *J. Phys. Oceanogr.*, **15**, 1369–1377.

Hasselmann, S., Hasselmann, K. Allender, J. H., and Barnett, T. P., 1985: Computations and parametrizations of the nonlinear energy transfer in a gravity-wave spectrum, Part II, Parameterizations of the nonlinear energy transfer for application in wave models, *J. Phys. Oceanogr.*, **15**, 1378–1391.

Hasselmann, K., D.B. Ross, P. Müller, and W. Sell, 1976: A parametric wave prediction model. *J. Phys. Oceanogr.*, **6**, 200-228.

Herterich, K., and K. Hasselmann, 1980: A similarity relation for the nonlinear energy transfer in a finite-depth gravity-wave spectrum, *J. Fluid Mech.*, **97**, 215-224.

Komen, G.J., Hasselmann, K., and S. Hasselmann, 1984: On the existence of a fully developed windsea spectrum, J. Phys. Oceanogr., **14**, 1271-1285.

Lin, R.Q., and W. Perrie, 1997: A new coastal wave model, III, Nonlinear wave-wave interactions for wave spectral evolution. *J. Phys. Oceanogr.* **27**, 1813-1826.

Lin, R.Q., and W. Perrie, 1999: Wave-wave interactions in finite depth water. *J. Geophys. Res.* **104** No. C5, 11193-11213.

Perrie, W., and D. Resio, 2004. Energy-Flux Balances and Source Term Parameterizations. Proc. 8th International Waves Workshop. Hawaii, 8pp.

Pettersson, H., Kahma, K.K., and L. Tuomi, 2004: Predicting wave directions in a narrow bay, submitted (7/11/2003) to *J. Phys. Oceanogr.*

Phillips, O.M., 1960: The dynamics of unsteady gravity waves of finite amplitude. *J. Fluid Mech.* **9**, 193-217.

Polnikov, V. G., 2002: A basing of the diffusion approximation derivation for the four-wave kinetic integral and properties of the approximation. *Nonlinear Processes in Geophys.* **9**, 355 – 366.

Pushkarev, A. N., D. Resio, D., and V. E. Zakharov, 2004:Second generation diffusion model of interacting gravity waves on the surface of deep fluid. *Nonlin. Processes Geophys.*, **11**, 329–342. SRef-ID: 1607-7946/npg/2004-11-329.

Resio, D.T., 1981: The estimation of wind-wave generation in a discrete spectral model. *J. Phys. Oceanogr.* **11**, 510-525.

Resio, D.T., C.E. Long, C. L. Vincent, 2004: Equilibrium-range constant in wind-generated wave spectra. *J. Geophys. Res.*., **109**, C01018, doi:10.1029/2003JC001788.

Resio, D. T. and W. Perrie, 1989: Implications of an f^{-4} equilibrium range for wind-generated waves, *J. Phys. Oceanogr.*, *19*, 193-204.

Resio, D. T. and W. Perrie, 1991: A numerical study of nonlinear energy fluxes due to wave-wave interactions. Part 1. Methodology and basic results, *J. Fluid Mech.*, **223**, 609-629.

Resio, D. T., J. H. Pihl, B. A. Tracy and C. L. Vincent, 2001: Nonlinear energy fluxes and the finite depth equilibrium range in wave spectra, *J. Geophys. Res.*, **106**, 6985-7000.

Tracy, B.A. and D.T. Resio, 1982: Theory and calculation of the nonlinear energy transfer between sea waves in deep water. WES rep. 11, US Army Engineer Waterways Exp. Sta., Vicksburg, MS.

Webb, D. J., 1978: Non-linear transfers between sea waves, Deep-Sea Res., **25**, 279–298.

Young, I.R. and H. Van Vledder, 1993: A review of the central role of nonlinear interactions in wind-wave evolution. Phil. Trans. Roy. Soc. London A, **342**, 505-524.

Zakharov, V. E. and N. N. Filonenko, 1966: The energy spectrum for stochastic oscillation of a fluid's surface, *Dokl. Akad. Nauk.*, **170**, 1992-1995.

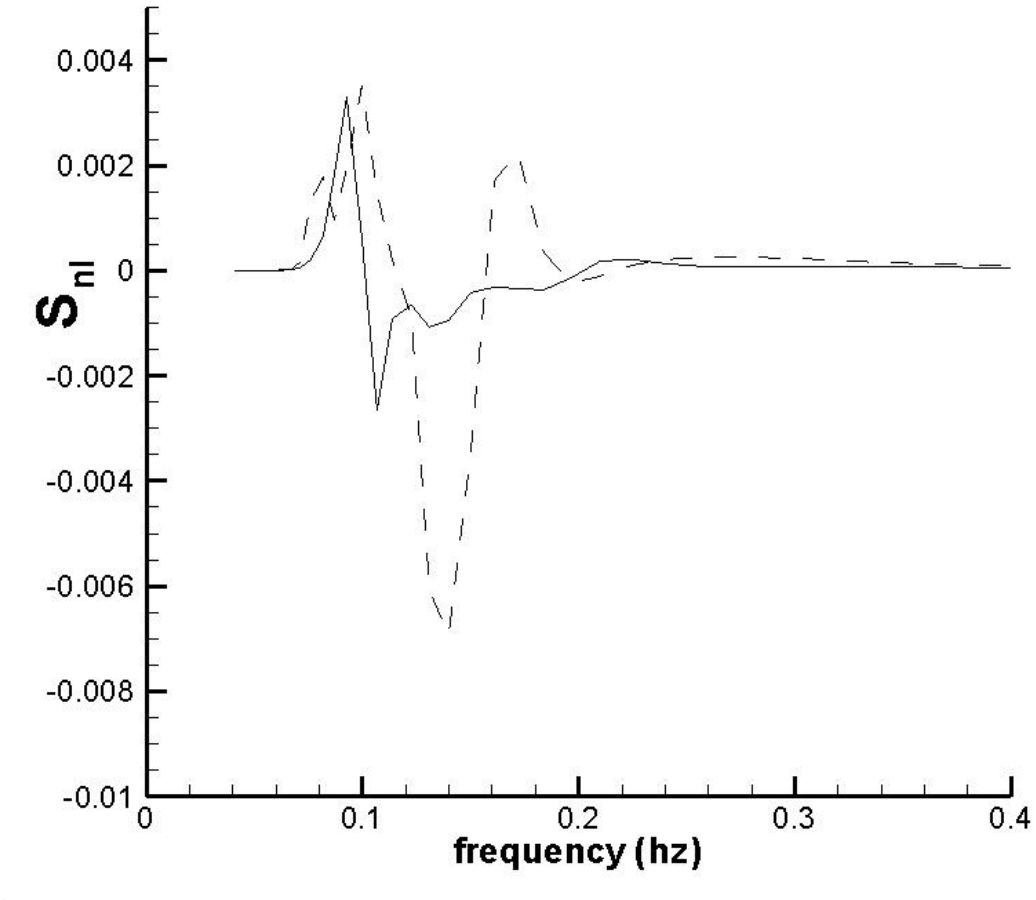

Figure 1. Comparison of the directionally integrated nonlinear interaction source term, $S_{nl}(f)$, for the DIA (dashed line) with results from the full Boltzmann integral (solid line) for a standard JONSWAP spectrum, with $\cos^4\theta$ angular distribution of energy around the central wave direction, and peak frequency f_p = 0.1 peakedness γ = 3.3.

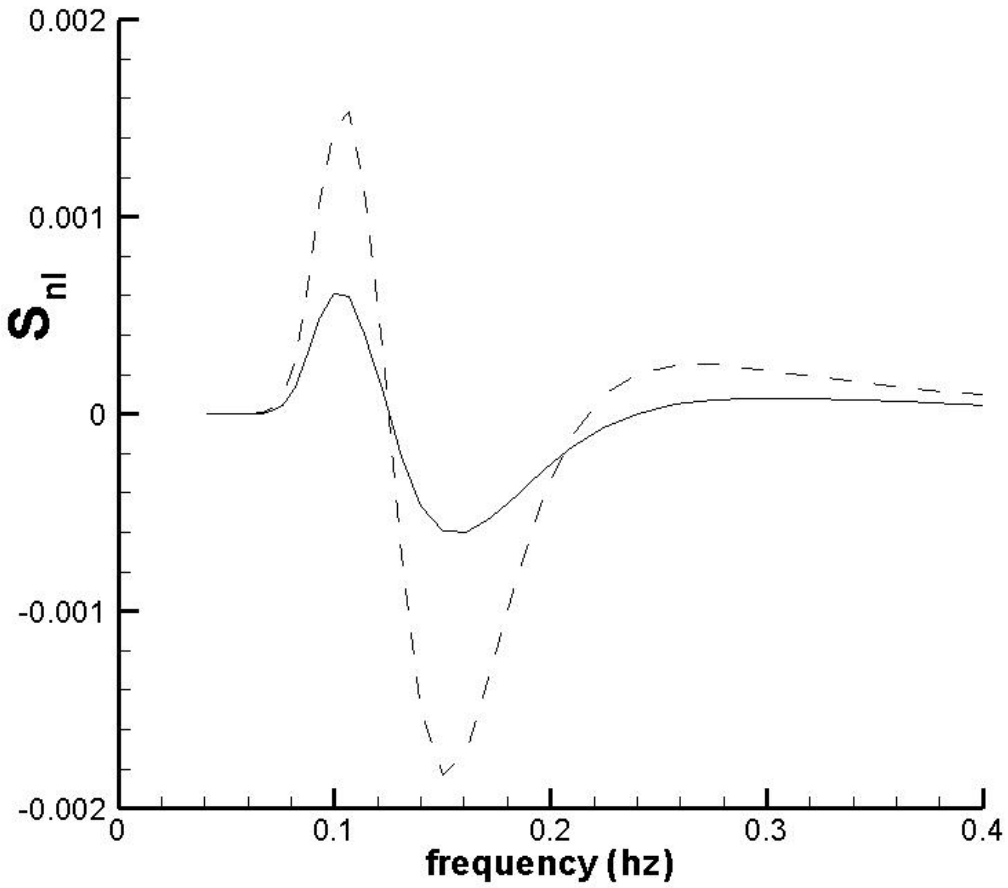

Figure 2. Comparison of the directionally integrated nonlinear interaction source term, $S_{nl}(f)$, for the DIA (dashed line) with results from the full Boltzmann integral (solid line) for a standard JONSWAP spectrum, with $\cos^4\theta$ angular distribution of energy around the central wave direction, and peak frequency $f_p = 0.1$ peakedness $\gamma = 1.0$.

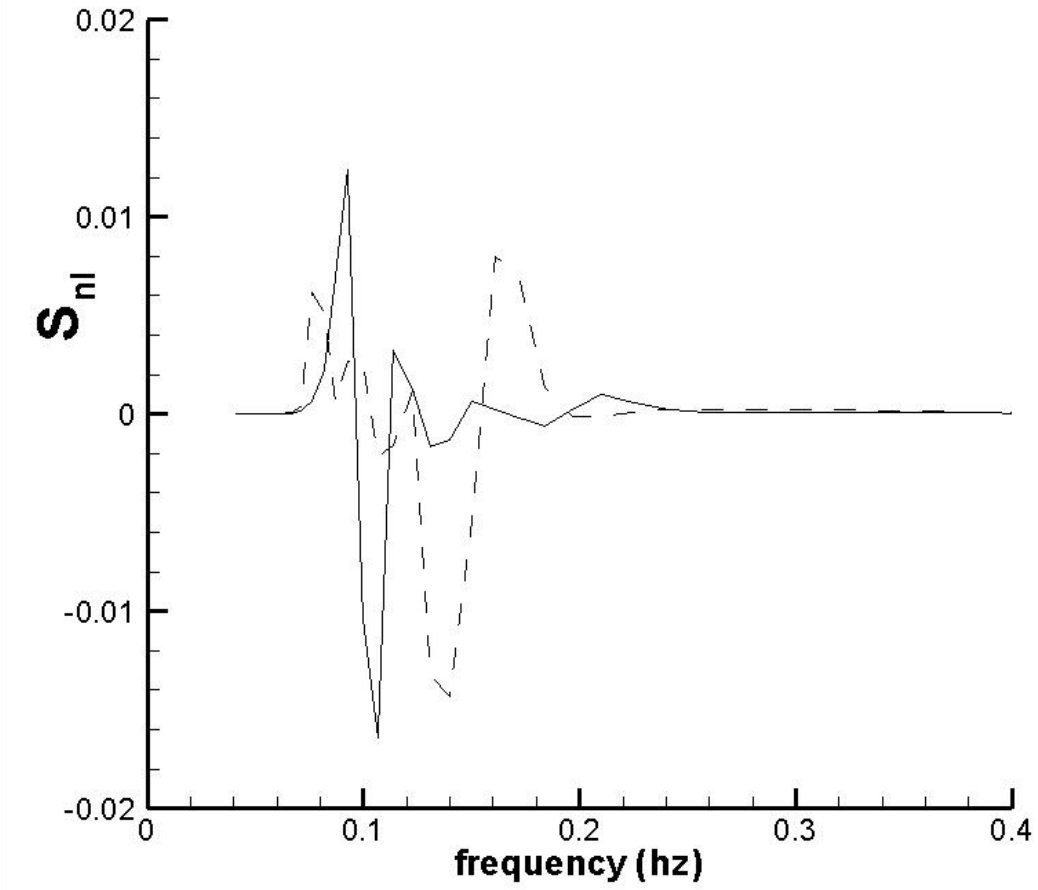

Figure 3. Comparison of the directionally integrated nonlinear interaction source term, $S_{nl}(f)$, for the DIA (dashed line) with results from the full Boltzmann integral (solid line) for a standard JONSWAP spectrum, with $\cos^4\theta$ angular distribution of energy around the central wave direction, and peak frequency $f_p = 0.1$ peakedness $\gamma = 7.0$.

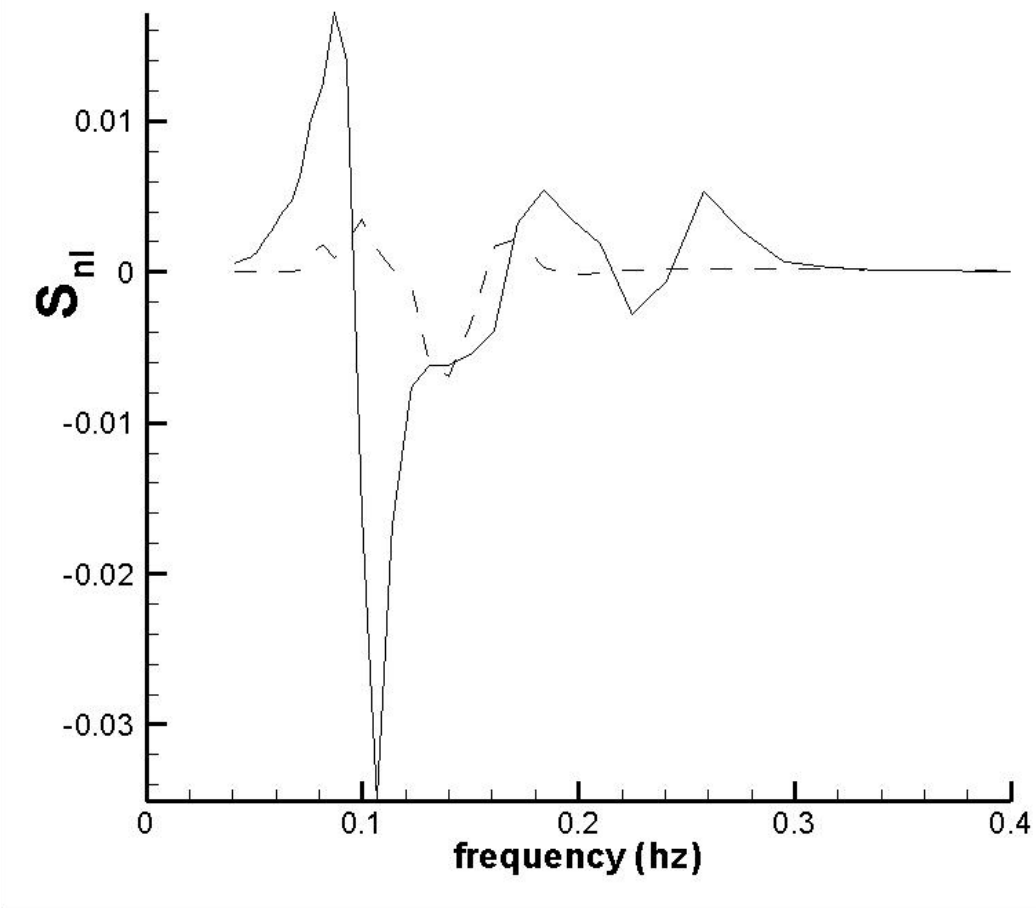

Figure 4. Comparison of a scaled DIA calculation and an actual full-integral, finite-depth calculation, showing that the scaled DIA estimate underestimates the positive lobe on the forward face of the spectrum by an order of magnitude for the case of $k_p h=0.7$ (JONSWAP spectrum with a peak period of 10 seconds in depth of 10.5 meters). The dashed line is the Herterich and Hasselmann (1980) scaling of the DIA and the solid line is the finite-depth, full integral solution for the same case.

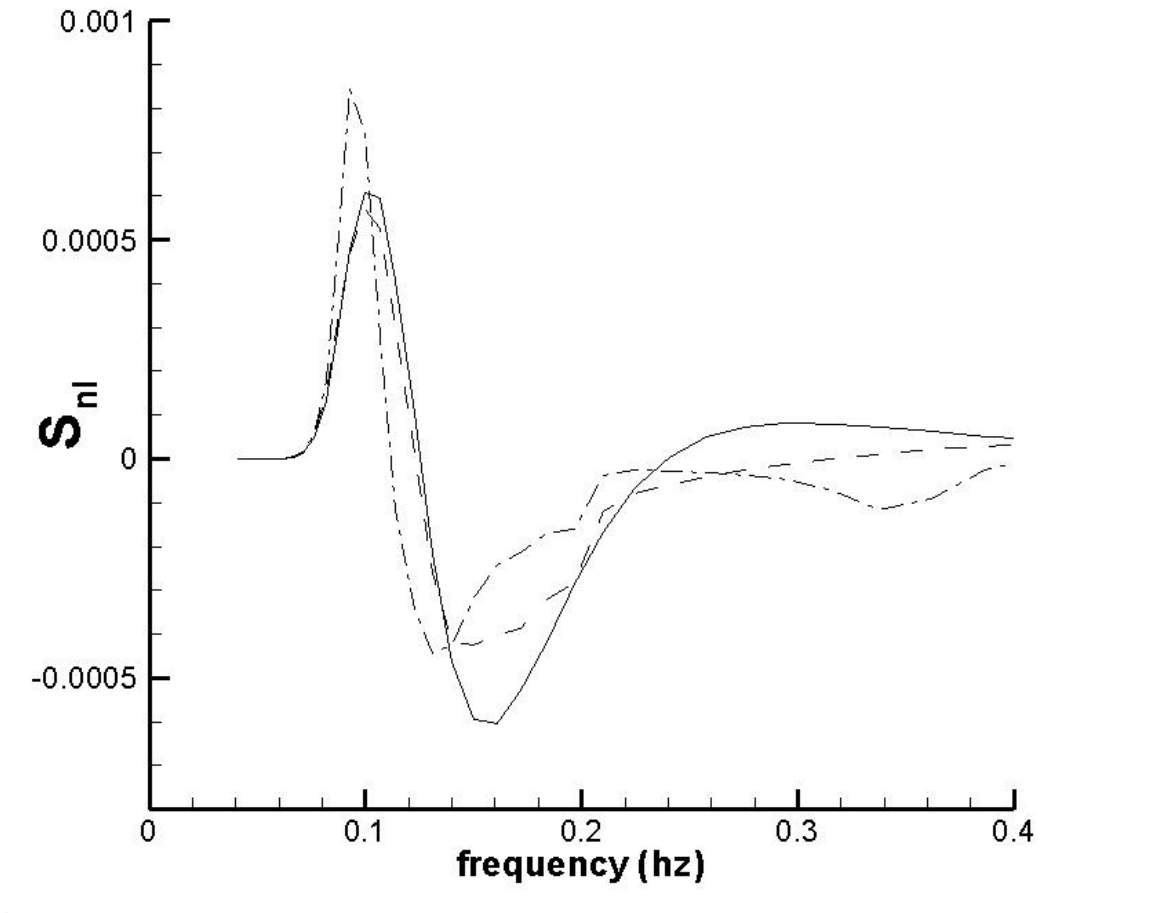

Figure 5. Comparisons of the TSA results to the full-integral solution for JONSWAP spectra with peakednesses equal to 1. Also shown is the contribution to the TSA from the parametric solution alone. (PM – solid full integral, dash TSA, dot-dash parametric alone).

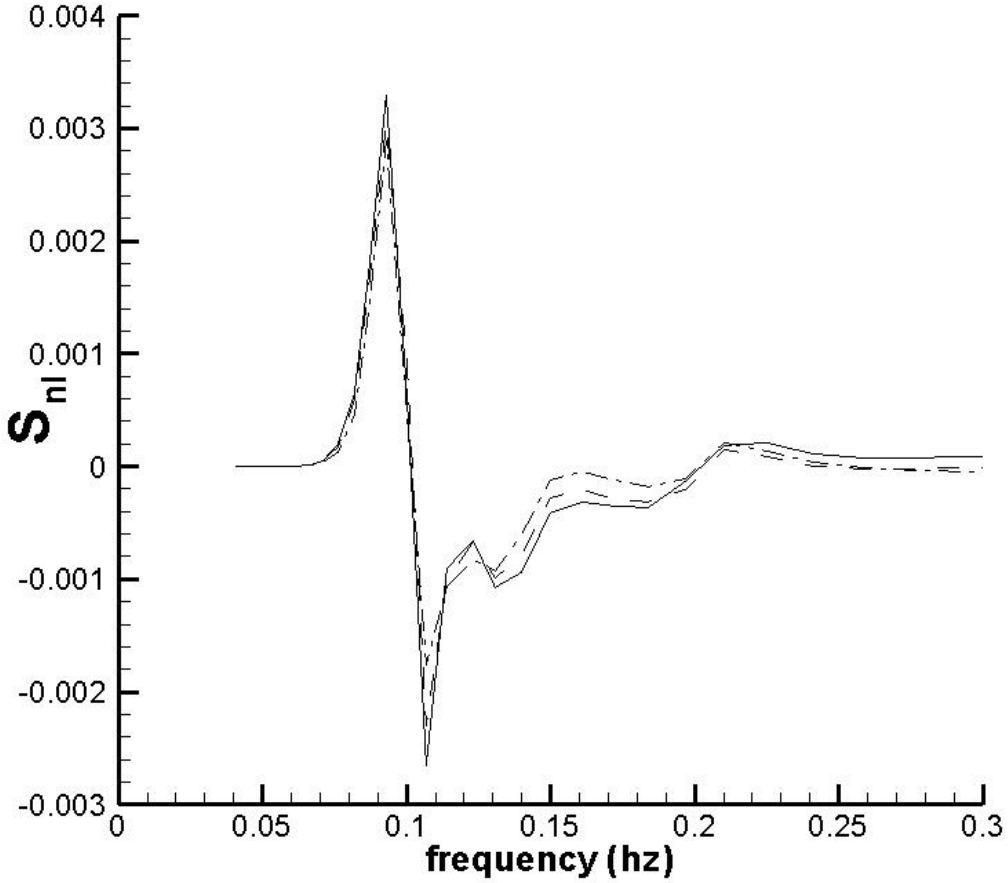

Figure 6. As in Figure 11a with peakednesses equal to 3.3.

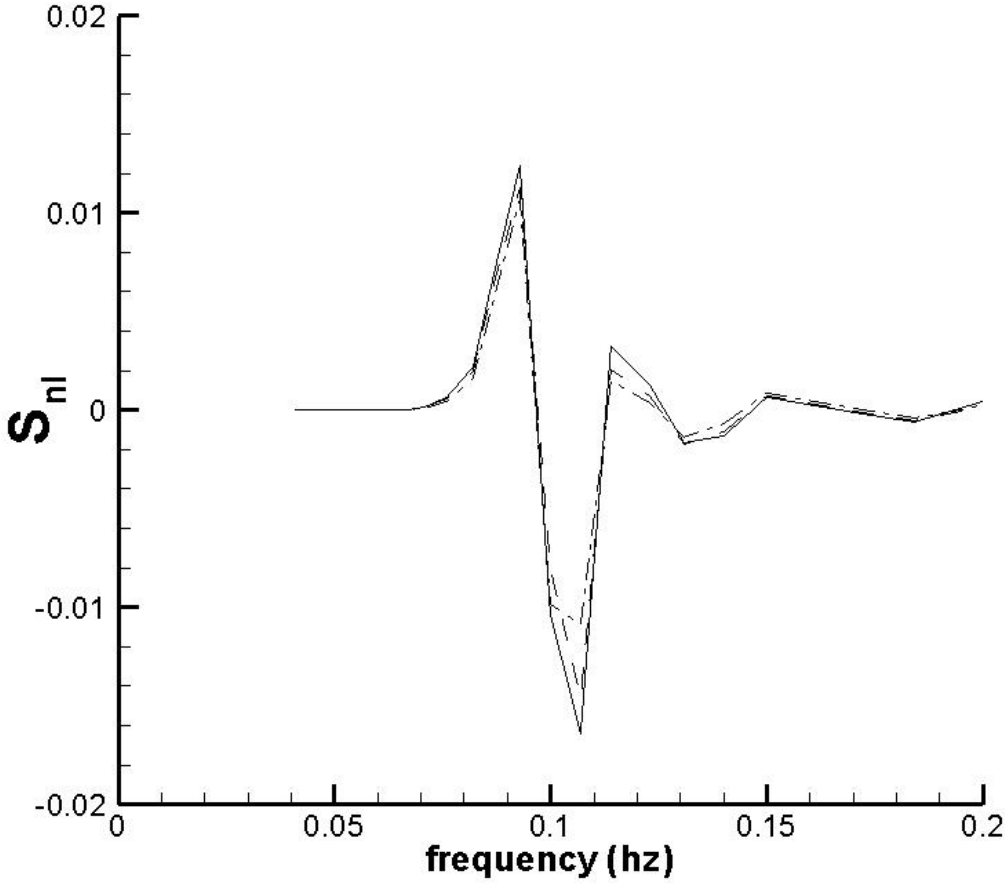

Figure 7. As in Figure 11a with peakednesses equal to 7.

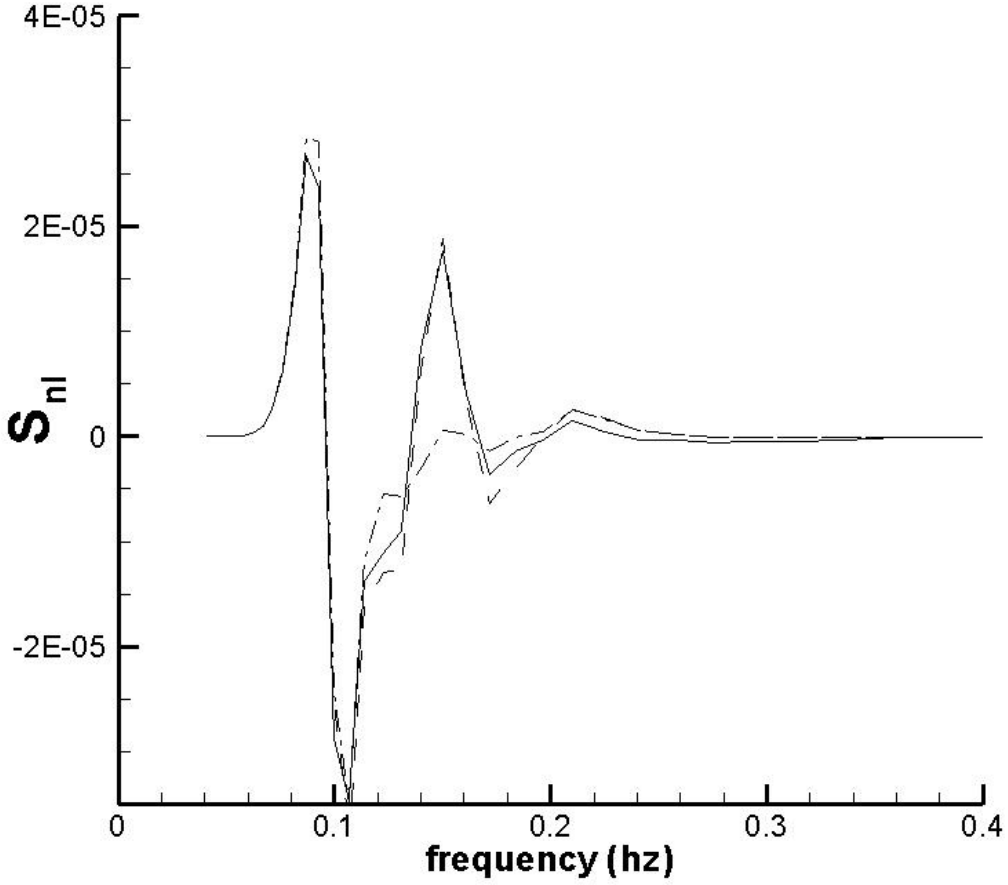

Figure 8. Results for (i) complete integral solution, (ii) parametric-only interactions, and (iii) TSA for the case of $\kappa = 2.2$ and a $\cos^4\theta$ angular spreading, with a secondary positive Gaussian perturbation superposed on the spectrum at $f / f_p = 1.5$, i.e. $A_z = 1$.

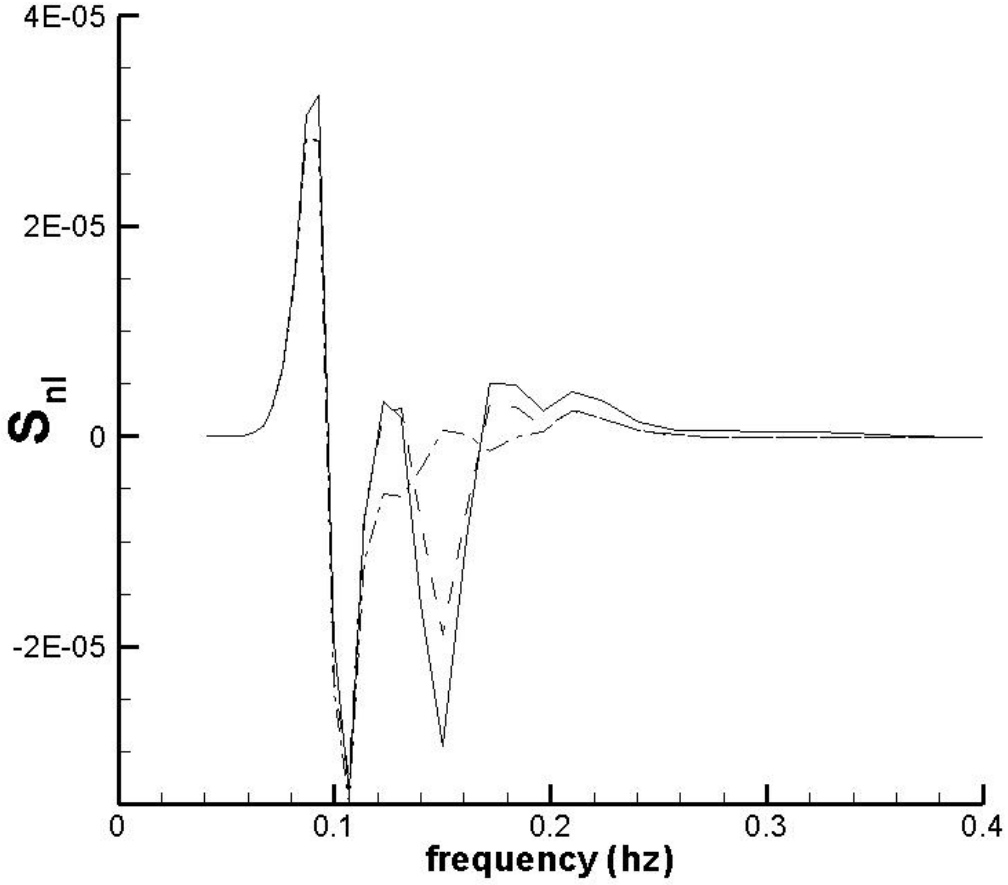

Figure 9. As in Figure 14a, for a negative Gaussian perturbation, i.e. $A_z = -1$.

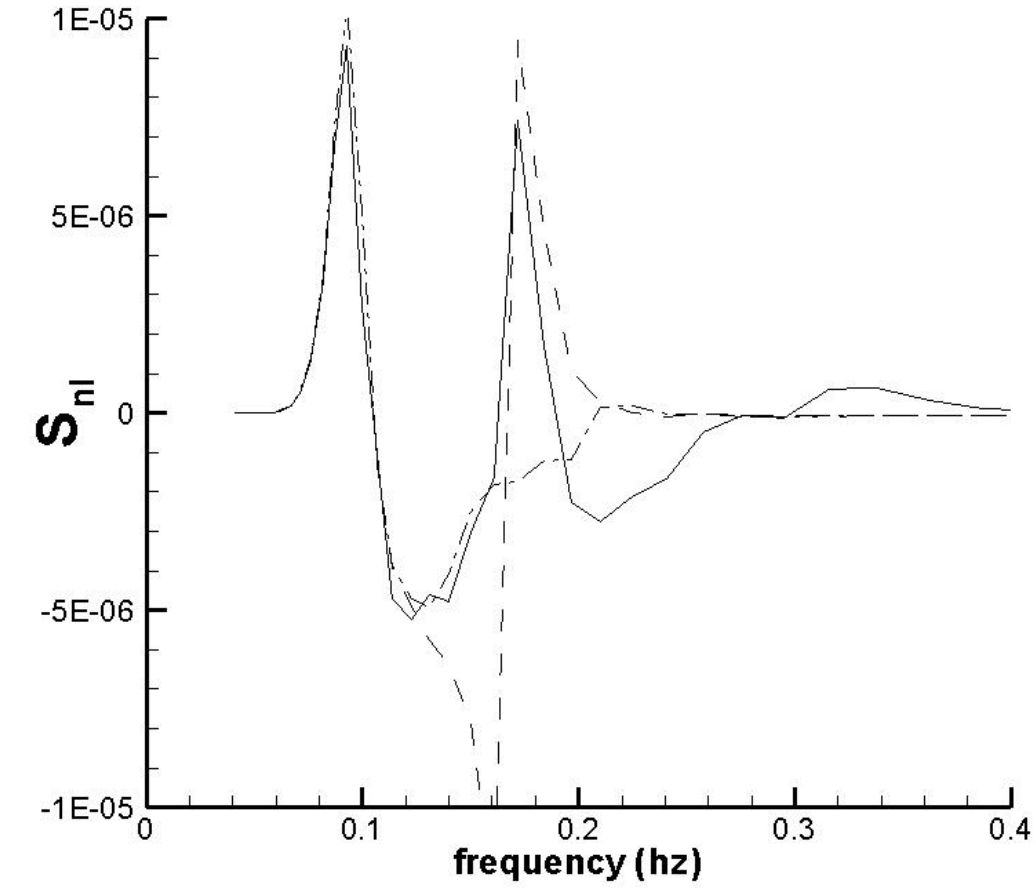

Figure 10. Results for a case in which the spectrum contains a 40-degree discontinuity at $f = 1.5 f_p$, retaining the same values for E(f) as though the spectrum had not been shifted. Case with 40-degree angle shift at 1.5 fp

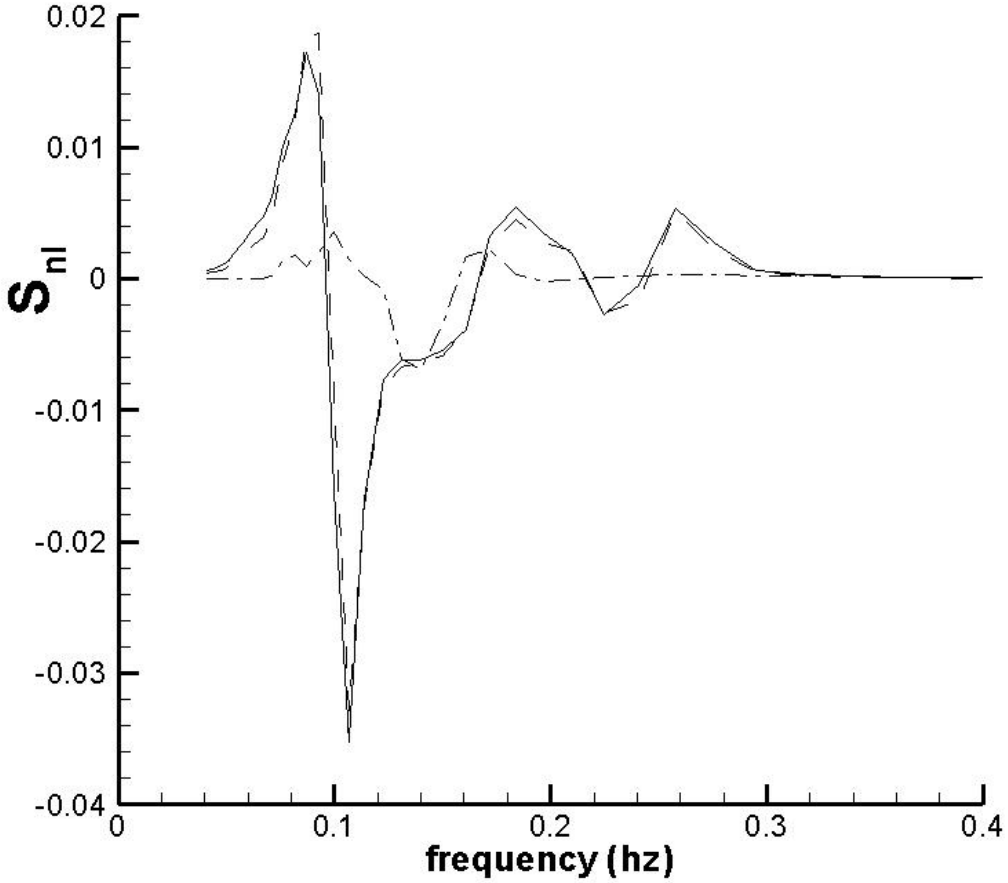

Figure 11. Results for the full-integral solution, TSA, and the DIA, using the actual depth of 10.5 meters. Finite depth kh=0.7 case, where solid line is full integral, dashed is TSA, and dot-dash is DIA.